A FAST RF STRUCTURE MONITOR*

Leonard M. DeBall and D. E. Suddeth
Argonne National Laboratory
Argonne, Illinois

Summary

A number of high energy physics experiments are based on a random distribution of particles entering the experimental apparatus. Unfortunately, the extracted beam from a proton synchrotron will display a bunching due to the RF cavity. However, this bunching can be reduced or destroyed by various techniques; such as, by introducing noise into the RF cavity during extraction, or by lengthening the energy loss target. Therefore, in order to measure the effectiveness of these various techniques, a monitoring system is needed to detect the amount of RF structure present in the extracted beam. The design of the RF structure monitor used at the Zero Gradient Synchrotron (ZGS) will now be described. Further, the results obtained from using this system will be discussed.

Introduction

Since the final accelerating frequency of the ZGS is 14 MHz, systems which can be used as an RF structure monitor are limited. These systems include a photomultiplier and a coincidence circuit with a real-time input and a delayed input; a photomultiplier with a time-to-amplitude converter and a pulse height analyzer; a toroid; and a resonant cavity. The system selected to be used at the ZGS is the photomultiplier with the coincidence circuit.

Extracted Beam Monitor

A block diagram of the complete extracted beam monitor, as it is called, appears in Fig. 1.

The design of the monitor is based on developing a voltage that is proportional to the amount of structure present. Since the intensity of the extracted beam varies from pulse to pulse, it is also necessary to develop a voltage that is proportional to the average beam intensity. Thus, the percentage of structure is given by

$$\%\ \text{structure} = \frac{\text{filter or structure voltage}}{\text{average beam voltage}} \times 100$$

100% corresponds to the case where the beam is fully coherent; and 0% corresponds to no structure.

To achieve a linear response to these two voltages, operational amplifiers are employed and identical configurations of amplifiers and integrators are used in both the numerator and the denominator channels whenever possible.

*Work performed under the auspices of the U. S. Atomic Energy Commission.

Photomultiplier

As is common for a structure measurement, a photomultiplier with a piece of scintillating plastic (Pilot B) is placed at right angles to one of the targets in each extracted proton beam line. The photomultiplier used is an Amperex type 56AVP. The logic circuits which receive the signal from this photomultiplier require that this signal have an amplitude of 2-3 V. The termination is 91 Ω. Thus, the peak current which must be furnished by the photomultiplier is 33 mA. Since the beam spill may be as long as 800 ms, the base for the photomultiplier had to be specially designed to supply fairly stable voltages to the dynodes for the entire beam spill. The maximum shift in the dynode voltages was set at 5 V. This degree of voltage regulation would easily have been achieved if transistor regulators or zener diodes could have been used. However, because the base would be operated in a high radiation area, these devices were excluded. Instead, a high current (20 mA) resistor divider and a set of large bypass capacitors were employed. The measured droop in the voltages of the last five dynodes was 2-4 V/dynode. The ouput pulse of the photomultiplier was found to have an amplitude of 2-3 V and a full-width at half-maximum of 12 ns using a 6 ns clipping line. The signal from the photomultiplier is fed to the extracted beam monitor display unit which is located in the Main Control Room (MCR) of the ZGS.

14 MHz Detection Circuit

A block diagram of the 14 MHz detection circuit is shown in Fig. 2.

The signal from the photomultiplier is fed into an EG & G Model TR104 discriminator. The main reason for this circuit is to discriminate against small voltage levels and low amplitude pulses. A problem which occurred when the monitor was tested was the induction of a small voltage in the coaxial cable of the monitor by the changing magnetic fields of the ZGS magnets. This small voltage when integrated caused errors in the data. Unfortunately, the cable had to be placed near the accelerator magnets in order to send the signal to the MCR. Therefore, a discriminator was employed to overcome this problem.

Another reason for the discriminator is the standardization of the pulses that are sent to x- and y-channels of the monitor display unit.

The y-channel, which generates the denominator term, consists of an amplifier and an integrator, and is used to obtain a voltage proportional to the average beam intensity. The x-channel, which generates the numerator term, consists of a 71 ns delay line, a coincidence circuit, an amplifier, and an integrator, and is used to develop a voltage that is proportional to the number of particles arriving at a 14 MHz rate. Both the amplifier and the integrator in the x-channel are identical to those used in the y-channel. Each integrator has an RC time constant of 0.8 µs. Further, both amplifiers and both integrators use Burr-Brown type 3400B operational amplifiers. The analog divider, which is a GPS type DIV501 unit, develops a voltage which is equal to the 14 MHz voltage divided by the average beam voltage. A meter is used to display the percentage.

Sample-and-Hold Circuit

Since the RF structure has been reported to vary during the spill, a sample-and-hold circuit has been incorporated in the display unit. A block diagram of this circuit is shown in Fig. 3. The sample time has been set to 100 ms. A toggle switch has been provided to bypass this circuit when it is not desired. One unique feature of this circuit is that it requires only one cable from the ZGS programmer to perform the two functions of sample and reset.

Additional Filters

The output of the average beam integrator contains not only a dc level, but also a number of low frequencies (frequencies < 1 MHz). Since these additional frequencies can be used as indicators of possible troubles with the accelerator, the output of this integrator is sent to other filters for further analysis.

The filters that have been incorporated are 50 Hz, 60 Hz, 120 Hz, 300 Hz, and 6-12 kHz. All filters are active bandpass types and are based on the negative immittance converter circuit.

A block diagram of the design used for the 120 Hz, 300 Hz, and 6-12 kHz filters is shown in Fig. 4. Each filter consists of a voltage follower for isolation, an active filter, a precision limiter, and an integrator. For changeability and ease of servicing, all of these stages for one frequency have been mounted on one printed circuit board. The output of the filter is sent to the x-input of the analog divider. To make the response of the y-channel similar to the x-channel, a precision limiter, an integrator, and an amplifier are added to the y-channel when these additional filters are used. The filters use 741 operational amplifiers. The slow integrators have a time constant of 10 ms.

Since 50 Hz and 60 Hz are relatively close, two active filters are cascaded in order to improve the selectivity. A block diagram of the design used for the 50 Hz and 60 Hz filters is shown in Fig. 5.

Division by Zero

When the extracted beam is not present, such as during acceleration or inversion, the voltages to both inputs of the analog divider are zero. Thus the output of the analog divider would be indeterminate. To prevent this, the comparator shown in Fig. 6 applies about 200 mV to the y-input (denominator) of the analog divider during the absence of the beam, and thereby the output of this stage is zero--as it should be.

Calibration

The 14 MHz detection circuit is calibrated by first nulling the 3400B operational amplifiers, then adjusting the length of the delay cable for a peak response at 14 MHz, and, finally, adjusting the pulse width cable of the TR104 discriminator for the desired bandpass. At the present time, the bandpass has been set to ± 2 MHz.

The calibration of the other filters is accomplished by injecting a sine wave voltage at the center frequency of each filter, and adjusting the gain control of the filter for a 100% reading.

Analysis

In a slow beam spill of about 600 ms, the 14 MHz structure varied from 10% at the start, to 8% for most of the spill, and then to 25% at the end. With the exception of the start of the spill, this behavior is in agreement with other methods of measurement. The slightly higher structure at the beginning is probably due to the RF cavity exerting greater control of the beam during initial targeting. After the beam strikes the targets, various feedback systems slow the radial movement of the beam.

The remaining filters showed 0% during this testing period. However, no troubles which would give any low-frequency structure were encountered with the machine at this time.

Conclusion

The design philosophy used in the RF structure monitor has been very successful. Work is now progressing on techniques to reduce the RF structure.

Acknowledgments

We wish to thank C. Potts, D. Jovanovic, and L. Ratner for their many helpful suggestions. We also wish to thank W. Czyz, A. Houston, D. Bohringer, S. Reinke, and J. Raiger for constructing the monitor.

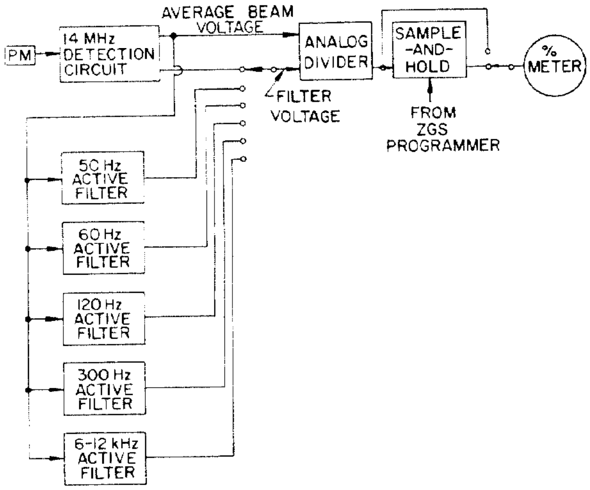

Fig. 1. Block Diagram of the Extracted Beam Monitor.

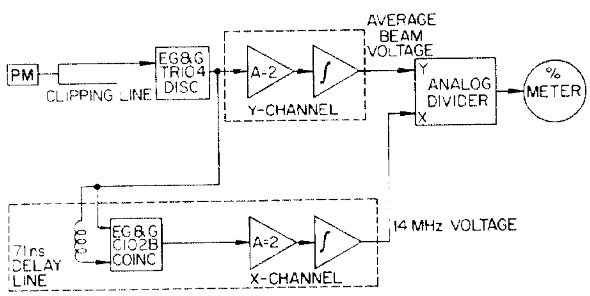

Fig. 2. Block Diagram of the 14 MHz Detection Circuit.

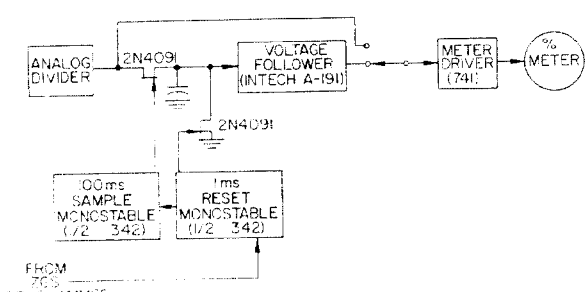

Fig. 3. Block Diagram of the Sample-and-Hold Circuit.

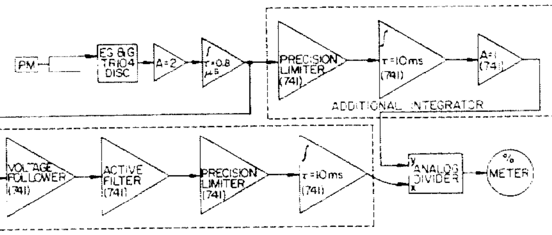

Fig. 4. Block Diagram of the Design Used for the 120 Hz, 300 Hz, and 6-12 kHz Filters.

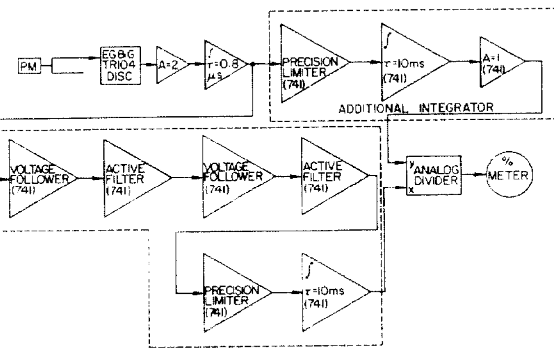

Fig. 5. Block Diagram of the Design Used for the 50 Hz and 60 Hz Filters.

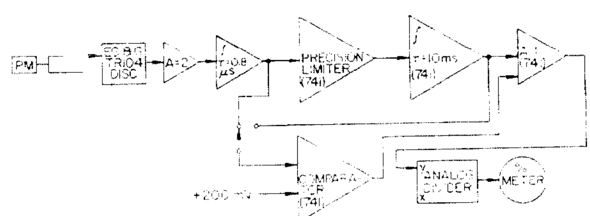

Fig. 6. Block Diagram of the Circuit Used to Suppress Division by Zero.